Nonlinear storage and retrieval of a multi-photon pulse in cold Rydberg atoms

Xue-Dong Tian[1,2], Yi-Mou Liu[1], Qian-Qian Bao[3], Jin-Hui Wu[1,*], M. Artoni[4], and G. C. La Rocca[5]
[1] *Center for Quantum Sciences, Northeast Normal University, Changchun 130117, P. R. China*
[2] *Department of Physics, Guangxi Normal University, Guilin 541004, P. R. China*
[3] *College of Physics, Liaoning University, Shenyang 110036, P. R. China*
[4] *European Laboratory for Nonlinear Spectroscopy (LENS), 50019 Firenze, Italy*
[5] *Scuola Normale Superiore and CNISM, 56126 Pisa, Italy and*
[*] *Corresponding author: jhwu@nenu.edu.cn*
(Dated: October 12, 2017)

We develop an effective method based on the superatom model to investigate the storage and retrieval of a multi-photon probe field in cold Rydberg atoms. This probe field is found greatly attenuated in light intensity and two-photon correlation yet suffering little temporal broadening as a result of the partial dipole blockade of Rydberg excitation. In particular, the output field energy exhibits a nontrivial saturation effect against the input field energy accompanied by a remarkable inhomogeneous anti-bunching feature as a manifestation of the dynamic cooperative optical nonlinearity. Our numerical results are quantitatively consistent with those in a recent experiment and may be extended to manipulate nonclassical light fields for quantum information applications.

PACS numbers: 42.50.Gy; 32.80.Ee; 42.65.-k

I. INTRODUCTION

Rydberg atoms [1] with a very large principal quantum number have exaggerated atomic properties including strong dipole-dipole interactions and long radiative lifetimes, which constitute the basis for many promising quantum information schemes and interesting quantum many-body effects. Such long-range interactions between atoms in a Rydberg state will cause a so-called blockade effect [2–6] that prohibits the simultaneous Rydberg excitation of two or more atoms in a mesoscopic volume. With this Rydberg blockade effect, significant advances have been achieved in quantum sciences, *e.g.*, on quantum entanglement [7–10], quantum gate [11–14], and quantum devices [15–21] including single-photon source, filter, absorber, switch, transistor, etc.

Many interesting phenomena, such as cooperative optical nonlinearity [22–25], nonlocal light propagation [26], bound states of photons [27, 28], and crystallization of atomic lattices [29], have been found when the long-range interaction between Rydberg atoms is combined with a famous quantum interference effect, electromagnetically induced transparency (EIT). Driving an ensemble of Rydberg atoms into the EIT regime also helps to implement nontrivial quantum devices like single-photon switch [19], single-photon transistor [20, 21], and cooperative nonlinear grating [30]. Quite recently, important experimental progresses have been achieved on light storage and retrieval in EIT media of cold [31, 32] or thermal [33] Rydberg atoms. It is found that a multi-photon pulse can be engineered to exhibit such peculiar properties as Rydberg mediated interactions [31] and two-photon states [34]. However, so far it still lacks a satisfactory theoretical method to recover relevant experimental results though several methods [35–38] have been proposed to deal with the the dynamic propagation of single-photon or few-photon pulses in Rydberg-EIT media.

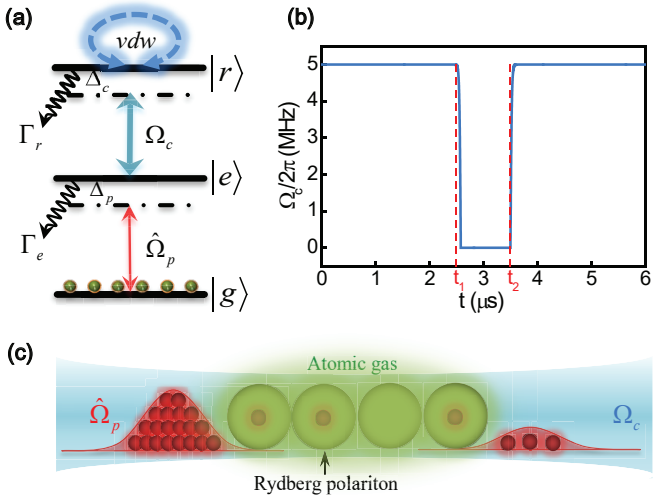

FIG. 1: (Color online) (a) Level configuration with the lower transition $|g\rangle \leftrightarrow |e\rangle$ probed by a quantum field of Rabi frequency $\hat{\Omega}_p$ and the upper transition $|e\rangle \leftrightarrow |r\rangle$ coupled by a classical field of Rabi frequency Ω_c. Vdw denotes the van der Waals interaction experienced by a pair of atoms in the Rydberg state $|r\rangle$. (b) Illustration of a coupling field turned off (on) at time t_1 (t_2) for realizing the storage and retrieval of a probe pulse. (c) Schematic representation of the input and output probe pulses separated by a sample of cold Rydberg atoms envisioned as a collection of superatoms.

In this paper, we study the storage and retrieval of a multi-photon probe pulse in a one-dimensional (1D) sample of cold Rydberg atoms in the EIT regime. Our calculations are based on a superatom (SA) model [22] extended here to be applicable also in the case of light propagation dynamics. One main finding is that the output probe pulse exhibits a negligible temporal broadening while its light intensity and two-photon correlation are severely attenuated. This corresponds to a partial

dipole blockade of Rydberg excitation, yielding a rough balance between the nonlinear loss for a two-level absorbing system and the linear loss for a three-level EIT system. Moreover, a nonlinear saturation effect and an inhomogeneous anti-bunching effect are found between the output and input field energies as a manifestation of the dynamic cooperative optical nonlinearity. Last but not least, an intermediate atomic density and a partial Rydberg blockade are required for attaining a bunch of single photons, otherwise more or less than one photon will be found in each blockade volume of SAs.

II. MODEL AND EQUATIONS

We consider a 1D sample of cold atoms driven into the three-level Ladder configuration as shown in Fig. 1(a) with a ground state $|g\rangle$, an excited state $|e\rangle$, and a Rydberg state $|r\rangle$. The lower transition $|g\rangle \leftrightarrow |e\rangle$ is probed by a quantum field of frequency ω_p and amplitude $\hat{\mathcal{E}}_p(z,t)$ while the upper transition $|e\rangle \leftrightarrow |r\rangle$ is coupled by a classical field of frequency ω_c and amplitude $E_c(t)$. Rabi frequencies (detunings) on the coupling and probe transitions are defined, respectively, as $\Omega_c(t) = E_c(t)\wp_{er}/2\hbar$ ($\Delta_c = \omega_c - \omega_{re}$) and $\hat{\Omega}_p(z,t) = g\hat{\mathcal{E}}_p(z,t)$ ($\Delta_p = \omega_p - \omega_{eg}$) with $g = \wp_{ge}\sqrt{\omega_p/(2\hbar\epsilon_0 V)}$ being the single-photon coupling strength, V the local quantum volume, $\omega_{re,eg}$ relevant transition frequencies, and $\wp_{er,ge}$ relevant electric dipole moments. In what follows, we will use $\hat{P}(z,t) = \sqrt{N}\hat{\sigma}_{ge}(z,t)$ and $\hat{S}(z,t) = \sqrt{N}\hat{\sigma}_{gr}(z,t)$ to describe the slowly-varying polarization and spin fields, *i.e*, continuum distributions of atomic excitations, with $\hat{\sigma}_{ge} = |g\rangle\langle e|$ and $\hat{\sigma}_{gr} = |g\rangle\langle r|$ being atomic transition operators while N the atomic volume density. The three optical or atomic fields coupled together satisfy the same-time commutation relations $[\hat{\mathcal{E}}_p(z,t), \hat{\mathcal{E}}_p^\dagger(z',t)] = [\hat{P}(z,t), \hat{P}^\dagger(z',t)] = [\hat{S}(z,t), \hat{S}^\dagger(z',t)] = \delta(z-z')$ in the limit of very low atomic excitations ($\hat{\sigma}_{gg} \to 1$).

In the frame rotating with frequencies $\omega_{p,c}$, we can write down the total Hamiltonian $\hat{\mathcal{H}} = \hat{\mathcal{H}}_p + \hat{\mathcal{H}}_{af} + \mathcal{H}_{int}$ including the kinetic term $\hat{\mathcal{H}}_p$, the atom-field coupling term $\hat{\mathcal{H}}_{af}$ and the interaction term $\hat{\mathcal{H}}_{int}$:

$$\hat{\mathcal{H}}_p = -c\int dz\hat{\mathcal{E}}_p^\dagger(z,t)\,\partial_z\hat{\mathcal{E}}_p(z,t), \tag{1a}$$

$$\begin{aligned}\hat{\mathcal{H}}_{ap} = &-\int dz[\Delta_p\hat{P}^\dagger(z,t)\,\hat{P}(z,t)\\ &+(\Delta_p+\Delta_c)\,\hat{S}^\dagger(z,t)\,\hat{S}(z,t)]\\ &-\int dz[g\hat{\mathcal{E}}_p(z,t)\,\hat{P}(z,t)\\ &+\Omega_c(t)\hat{S}^\dagger(z,t)\,\hat{P}(z,t)+h.c.],\end{aligned} \tag{1b}$$

$$\begin{aligned}\hat{\mathcal{H}}_{int} = &\frac{1}{2}\int dz\int dz'\hat{S}^\dagger(z,t)\,\hat{S}^\dagger(z',t)\\ &\Delta(z-z')\,\hat{S}(z',t)\,\hat{S}(z,t)\end{aligned} \tag{1c}$$

where we have considered that a pair of atoms i and j located at positions z_i and z_j simultaneously excited to the Rydberg state $|r\rangle$ interact with each other via a vdW potential $\Delta(z_i - z_j) = C_6/|z_i - z_j|^6$.

Using Hamiltonian $\hat{\mathcal{H}}$, it is then straightforward to obtain the Heisenberg-Langevin equations:

$$\begin{aligned}\partial_t\hat{P}(z,t) = &-(\gamma_e + i\Delta_p)\hat{P}(z,t)\\ &-i\Omega_c(t)\hat{S}(z,t) - i\hat{\Omega}_p(z,t),\end{aligned} \tag{2a}$$

$$\begin{aligned}\partial_t\hat{S}(z,t) = &-[\gamma_r + i(\Delta_p + \Delta_c - \langle\hat{\Delta}_s\rangle)]\hat{S}(z,t)\\ &-i\Omega_c(t)\hat{P}(z,t),\end{aligned} \tag{2b}$$

$$\partial_t\hat{\Omega}_p(z,t) = -c\partial_z\hat{\Omega}_p(z,t) + ig\sqrt{N}\hat{P}(z,t) \tag{2c}$$

where $\hat{\Delta}_s = \frac{1}{2}\int dz\int dz'\hat{S}^\dagger(z',t)\Delta(z-z')\hat{S}(z',t)\hat{S}(z,t)$ is the vdW-induced frequency shift while γ_e (γ_r) is the coherence dephasing rate on transition $|g\rangle \leftrightarrow |e\rangle$ ($|e\rangle \leftrightarrow |r\rangle$). Langevin noises have been omitted here as it does not affect our calculations. To solve these coupled equations, we then introduce the terminology of SA defined as $n_{SA} = NV_{SA}$ atoms in the blockade volume $V_{SA} = 4\pi R_b^3/3$ of radius $R_b \approx [C_6\gamma_e/(|\Omega_c(t)|^2 + \gamma_e\gamma_r)]^{1/6}$ [39]. In the mean field sense, the expected value $\langle\hat{\Delta}_s\rangle$ tends to infinite (vanishing) for the atoms in such SAs with (without) a definite Rydberg excitation, whereas vdW interactions between different SAs are typically very weak and can be qualitatively described by a small dephasing rate γ_s and a small frequency shift δ_s [39, 40].

With above considerations, it it clear that the atoms in such SAs with (without) a definite Rydberg excitation behave like a two-level (three-level) system excluding (including) the Rydberg state $|r\rangle$. In the more general case, however, each atom should behave like a superposition of two-level and three-level systems determined solely by the probability of finding a single Rydberg excitation in relevant SAs. In this regard, the dynamic equations of polarization and spin fields can be rewritten as

$$\begin{aligned}\partial_t\hat{P}_3(z,t) = &-(\gamma_e + i\Delta_p)\hat{P}_3(z,t)\\ &-i\Omega_c(t)\hat{S}_3(z,t) - i\hat{\Omega}_p(z,t),\end{aligned} \tag{3a}$$

$$\begin{aligned}\partial_t\hat{S}_3(z,t) = &-[\gamma_r + i(\Delta_p + \Delta_c)]\hat{S}_3(z,t)\\ &-i\Omega_c(t)\hat{P}_3(z,t)\end{aligned} \tag{3b}$$

for the three-level system and

$$\partial_t\hat{P}_2(z,t) = -(\gamma_e + i\Delta_p)\hat{P}_2(z,t) - i\hat{\Omega}_p(z,t) \tag{4}$$

for the two-level system.

To further determine the single Rydberg-excitation probability in relevant SAs, we then introduce as usual the first-order collective states $|G\rangle = |g_1, ...g_i, ...g_{n_{SA}}\rangle$, $|E^{(1)}\rangle = 1/\sqrt{n_{SA}}\sum_j^{n_{SA}}|g_1, ...e_i, ...g_{n_{SA}}\rangle$ and $|R^{(1)}\rangle = 1/\sqrt{n_{SA}}\sum_j^{n_{SA}}|g_1, ...r_i, ...g_{n_{SA}}\rangle$. Other higher-order collective states originating from $|E^{(1)}\rangle$ can be safely neglected if we choose to work at the center of an EIT window where the excitation to $|E^{(1)}\rangle$ is well suppressed

due to quantum destructive interference [25]. Accordingly, we can define $\hat{\Sigma}_{IJ} = |I\rangle\langle J|$ as the collective transition ($I \neq J$) or projection ($I = J$) operators with $\{I, J\} \in \{G, E^{(1)}, R^{(1)}\}$, whose dynamic evolution obey the following equations

$$\begin{aligned}
\partial_t\hat{\Sigma}_{GG}(z,t) &= 2\gamma_e\hat{\Sigma}_{EE}(z,t) - i\sqrt{n_{SA}}\hat{\Omega}_p(z,t)\hat{\Sigma}_{GE}(z,t) \\
&\quad + i\sqrt{n_{SA}}\hat{\Omega}_p^\dagger(z,t)\hat{\Sigma}_{EG}(z,t), \\
\partial_t\hat{\Sigma}_{EE}(z,t) &= -2\gamma_e\hat{\Sigma}_{EE}(z,t) + 2\gamma_r\hat{\Sigma}_{RR}(z,t) \\
&\quad - i[\Omega_c(t)\hat{\Sigma}_{ER}(z,t) - \Omega_c^*(t)\hat{\Sigma}_{RE}(z,t)] \\
&\quad + i\sqrt{n_{SA}}\hat{\Omega}_p(z,t)\hat{\Sigma}_{GE}(z,t) \\
&\quad - i\sqrt{n_{SA}}\hat{\Omega}_p^\dagger(z,t)\hat{\Sigma}_{EG}(z,t), \\
\partial_t\hat{\Sigma}_{GE}(z,t) &= -(\gamma_e + i\Delta_p)\hat{\Sigma}_{GE}(z,t) - i\Omega_c(t)\hat{\Sigma}_{GR}(z,t) \\
&\quad + i\sqrt{n_{SA}}\hat{\Omega}_p^\dagger(z,t)[\hat{\Sigma}_{EE}(z,t) - \hat{\Sigma}_{GG}(z,t)], \\
\partial_t\hat{\Sigma}_{GR}(z,t) &= -(\gamma_r + i\Delta_p + i\Delta_c)\hat{\Sigma}_{GR}(z,t) \\
&\quad - i\Omega_c^*(t)\hat{\Sigma}_{GE}(z,t) \\
&\quad + i\sqrt{n_{SA}}\hat{\Omega}_p^\dagger(z,t)\hat{\Sigma}_{ER}(z,t), \\
\partial_t\hat{\Sigma}_{ER}(z,t) &= -(\gamma_e + \gamma_r + i\Delta_c)\hat{\Sigma}_{ER}(z,t) \\
&\quad + i\Omega_c^*(t)[\hat{\Sigma}_{RR}(z,t) - \hat{\Sigma}_{EE}(z,t)] \\
&\quad + i\sqrt{n_{SA}}\hat{\Omega}_p^\dagger(z,t)\hat{\Sigma}_{GR}(z,t),
\end{aligned} \tag{5}$$

constrained by $\hat{\Sigma}_{GG} + \hat{\Sigma}_{EE} + \hat{\Sigma}_{RR} = 1$ and $\hat{\Sigma}_{IJ} = \hat{\Sigma}_{JI}^\dagger$. These equations are similar to those for atomic transition or projection operators $\hat{\sigma}_{ij}$ with $\{i, j\} \in \{g, e, r\}$ except $\hat{\Omega}_p(z,t)$ has been replaced by $\sqrt{n_{SA}}\hat{\Omega}_p(z,t)$. In the case of a very large n_{SA}, the Rydberg-excitation probability $\langle\hat{\Sigma}_{RR}\rangle$ in a SA should be much larger than its atomic counterpart $\langle\hat{\sigma}_{gg}\rangle$ so that it is not negligible even for a very weak probe field.

Solving Eq. (3)-Eq. (5) together it is then possible to attain the conditional probe polarizability

$$\begin{aligned}
\hat{P}(z,t) &= \hat{P}_2(z,t)\langle\hat{\Sigma}_{RR}(z,t)\rangle \\
&\quad + \hat{P}_3(z,t)(1 - \langle\hat{\Sigma}_{RR}(z,t)\rangle)
\end{aligned} \tag{6}$$

with the consideration that the two-photon correlation $g_p^{(2)}(z,t) = \frac{\langle\hat{\mathcal{E}}_p^\dagger(z,t)\hat{\mathcal{E}}_p^\dagger(z,t)\hat{\mathcal{E}}_p(z,t)\hat{\mathcal{E}}_p(z,t)\rangle}{\langle\hat{\mathcal{E}}_p^\dagger(z,t)\hat{\mathcal{E}}_p(z,t)\rangle\langle\hat{\mathcal{E}}_p^\dagger(z,t)\hat{\mathcal{E}}_p(z,t)\rangle}$ should be introduced to answer for the modification of photon statistics conditioned upon Rydberg blockade. That is, we should replace $\hat{\Omega}_p^\dagger(z,t)\hat{\Omega}_p(z,t)$ with $\langle\hat{\Omega}_p^\dagger(z,t)\hat{\Omega}_p(z,t)\rangle g_p^{(2)}(z,t)$ to reserve the two-particle quantum correlation arising from the vdW interaction. Accordingly, the dynamic evolution of a probe pulse this Rydberg-EIT medium is governed by the following two coupled equations

$$\partial_z\Omega_p(z,t) = \frac{i\omega_p\wp_{ge}^2\sqrt{N}}{2\hbar\epsilon_0 c}P(z,t), \tag{7a}$$

$$\begin{aligned}
\partial_z g_p^{(2)}(z,t) &= \frac{-\omega_p\wp_{ge}^2\sqrt{N}}{\hbar\epsilon_0 c}\Sigma_{RR}(z,t) \\
&\quad [\frac{P_2(z,t) - P_3(z,t)}{\Omega_p(z,t)}]g_p^{(2)}(z,t),
\end{aligned} \tag{7b}$$

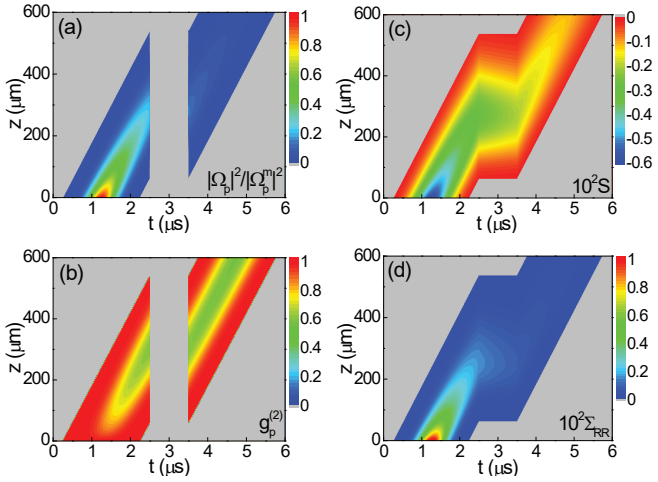

FIG. 2: (Color online) Dynamic evolution of the scaled light intensity (a), the two-photon correlation (b), the atomic spin field (c), and the SA Rydberg population (d) for an input probe pulse in the coherent state described by $\Omega_p(0,t) = \Omega_p^m e^{-(t-t_0)^2/\delta t^2}$ and $g_p^{(2)}(0,t) = 1.0$. Relevant parameters are given at the beginning of section III except $\Omega_p^m/2\pi = 0.03$ MHz, $t_0 = 1.25\ \mu s$, and $\delta t = 0.5\ \mu s$.

where $O(z,t) = \langle\hat{O}(z,t)\rangle$ has been used to represent the expectation value of operator $\hat{O}(z,t)$. We have also considered that $g_p^{(2)}(z,t)$ is determined by the nonlinear absorption with the linear one excluded.

III. RESULTS AND DISCUSSION

In this section, we implement numerical calculations by modulating the coupling field [see Fig. 1(b)] to study light storage and retrieval [see Fig. 1(c)] in a Rydberg-EIT medium of length $L = 600\ \mu m$ and density $N = 7.5\times10^{11}$ cm^{-3}. We assume, in particular, $|g\rangle \equiv |5S_{1/2}, F = 2\rangle$, $|e\rangle \equiv |5P_{3/2}, F = 3\rangle$, and $|r\rangle \equiv |60S_{1/2}\rangle$ for cold ^{87}Rb atoms. Then we have $\gamma_e = 3.0\times2\pi$ MHz, $\gamma_r = 2.0$ kHz, and $C_6 = 1.4\times10^{11}\times2\pi\ s^{-1}\mu m^{-1}$. In reference to a practical experiment, the one- and two-photon laser linewidths $\delta\omega_{1,2} \simeq (5, 10)\times10^4\ s^{-1}$ [22] need to be included in the dephasing rates so that we have $\gamma_e \to \gamma_e + \delta\omega_1$ and $\gamma_r \to \gamma_r + \delta\omega_2$ for the transition operators. In addition, we choose to always work in the EIT regime characterized by $\Delta_p = \Delta_c = 0$ though the coupling field with $\Omega_c = 5\times2\pi$ MHz will be adiabatically turned off (on), *e.g.*, at $t_1 = 2.5\ \mu s$ ($t_2 = 3.5\ \mu s$). In this case, each SA contains on average $n_{SA} \simeq 295$ ($\simeq 700$) atoms with the blockade radius $R_b \simeq 5\ \mu m$ ($\simeq 12\ \mu m$) when the coupling field is on (off). A dephasing rate γ_s and a frequency shift δ_s (both estimated as a few tens of kHz) arising from the vdW interactions between different SAs [39, 40] will also be included in our calculations.

We first check in Fig. 2 how the light intensity, the two-photon correlation, the atomic spin wave, and the SA

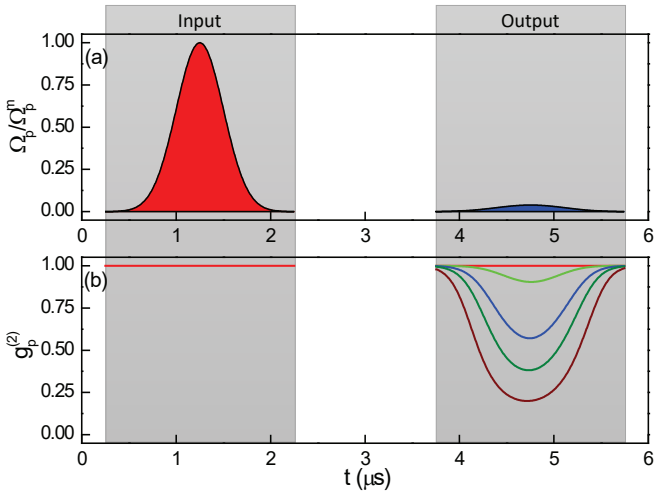

FIG. 3: (Color online) Intensity profile (a) and two-photon correlation (b) of a quantum probe field at the sample entrance (left) and exit (right) as a function of time. Relevant parameters are the same as in Fig. 2 except $\Omega_p^m/2\pi = 0.001$ MHz, 0.01 MHz, 0.03 MHz, 0.05 MHz, and 0.1 MHz for the five curves in the lower right panel from top to bottom.

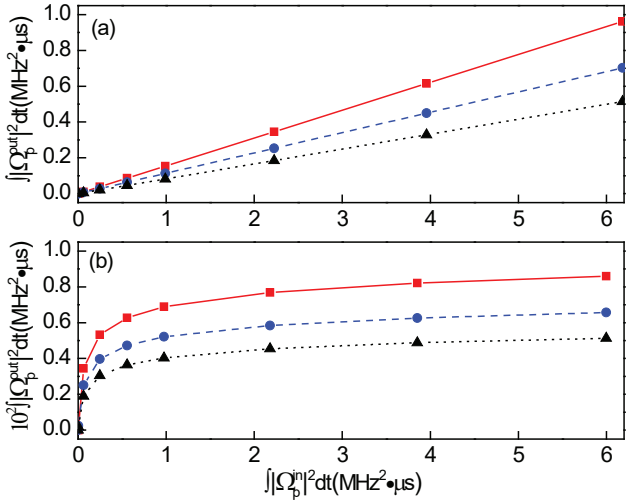

FIG. 4: (Color online) Output field energy versus input field energy in the absence (a) or presence (b) of a vdW interaction. The red-solid, blue-dashed, and black-dotted curves correspond to a storage times of 0.0 μs, 0.5 μs, and 1.0 μs, respectively. Other parameters are the same as in Fig. 2 except $\Omega_p^m/2\pi$ is increased from zero until 0.5 MHz.

Rydberg population evolve during the storage-retrieval process in a Rydberg-EIT medium for a weak probe pulse in the coherent state. It is clear that the four quantities are tightly coupled and propagate together at a group velocity $v \approx 240\ m/s$ when the coupling field is on. This indicates the formation of a Rydberg dark-state polariton (RDP) defined here by $\Psi(z,t) = \cos\theta(t)\Omega_p(z,t) - \sin\theta(t)S(z,t)$ with $\tan\theta(t) = g\sqrt{N}/\Omega_c(t)$. When the coupling field is off, the probe field is completely mapped onto the spin field so that the RDP becomes stationary in the medium. Above findings are *trivial* because they are typically found when we study light storage and retrieval in cold atoms without a Rydberg state. Two *nontrivial* findings are given below. First, light intensity, two-photon correlation, and spin field suffer severe dissipation before the coupling field is turned off while experience little change after the coupling field is turned on. This is because the two-level polarization P_2 plays a significant (immaterial) role in the presence of remarkable (negligible) SA Rydberg population in the first (second) stage. Second, the losses in light intensity, two-photon correlation, and spin field are temporally/spatially inhomogeneous because the Rydberg excitation depends critically on the local intensity and correlation of probe pulse. Note also that a SA Rydberg population $\Sigma_{rr} \sim 0.01$ is already enough to result in an obvious blockade effect. So the Rydberg blockade effect in the dynamic case for a pulsed field exhibits clearly different characteristics as compared to that in the steady case for a cw field.

Then we compare the input and output probe fields by plotting in Fig. 3 the intensity profile and the two-photon correlation as a function of time. Fig. 3(a) shows that the output probe field is greatly attenuated as compared to the input probe field yet without exhibiting an evident temporal broadening (from 1.85 μs to 1.89 μs in full width at half maximum). On the contrary, a severe intensity attenuation is typically accompanied by a large temporal broadening for a weak pulse slowly traveling in the usual EIT media. This indicates that the linear absorption contributed by P_3 of weight $1 - \Sigma_{rr}$ and the nonlinear absorption contributed by P_2 of weight Σ_{rr} are roughly comparable to result in a balanced effect on the probe frequencies at both wings and those at the center of the EIT window. That is, the probe field loses its sideband (central) frequencies mainly due to the linear (nonlinear) absorption. Fig. 3(b) shows that the modification of photonic statistics becomes evident for a probe pulse with its maximal amplitude as low as $\Omega_p^m = 0.01$ MHz, and the inhomogeneous two-photon correlation exhibits a stronger and stronger anti-bunching effect at the pulse center as Ω_p^m is gradually increased. This is consistent with relevant results in ref. [22] where the modification of two-photon correlation is shown to depend on the input intensity of a cw probe field. Note, however that square probe pulses may be adopted to attain a homogeneous modification of two-photon correlation and thus a bunch of single photons with $g_P^{(2)} \to 1$.

Considering the photon number is proportional to the field energy, we further plot in Fig. 4 the output field energy $I_p^{out} = \int|\hat{\Omega}_p(L,t)|^2 dt$ versus the input field energy $I_p^{in} = \int|\hat{\Omega}_p(0,t)|^2 dt$ to verify that there is a restriction on the maximal number of stored probe photons. Fig. 4(a) displays that I_p^{out} varies linearly with the increase of I_p^{in} in the absence of a vdW interaction; about 15.5%, 11.4%, and 8.3% probe photons survive at the sample exit due to the linear absorption contributed only by P_3 for the

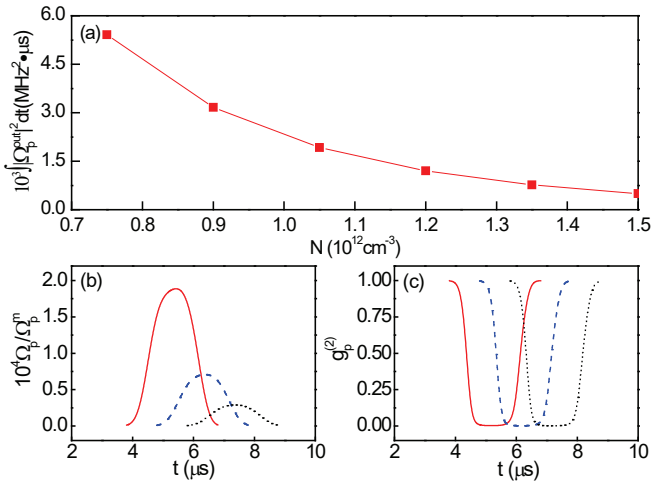

FIG. 5: (Color online) (a) Saturation value of output field energy versus atomic density. (b) Intensity profile and (c) two-photon correlation of output field as a function of time for $N = 0.9 \times 10^{12}$ cm^{-3} (red-solid); $N = 1.2 \times 10^{12}$ cm^{-3} (blue-dashed); $N = 1.5 \times 10^{12}$ cm^{-3} (black-dotted). Other parameters are the same as in Fig. 2 except suitable values of $\Omega_p^m/2\pi$ are chosen to attain the saturation effect.

storage times 0.0 μs, 0.5 μs, and 1.0 μs, respectively. Fig. 4(b) displays that I_p^{out} varies in a nonlinear way as I_p^{in} is increased in the presence of a vdW interaction; the saturation values of 0.14%, 0.11%, and 0.086% survived probe photons are found for the storage times 0.0 μs, 0.5 μs, and 1.0 μs, respectively. Such a nonlinear behavior is a direct result of Rydberg blockade, which prohibits the storage of more than one photon in a blockade volume. That is, as the input field energy increases, each SA get a larger probability to have one Rydberg excitation so that the traveling probe photons suffers more nonlinear absorption. This is why the same increase of input field energy leads to less and less increase of output field energy until the stored photon number reaches a saturation value. In other words, the number of stored photons is restricted by the number of SAs in a Rydberg-EIT medium. It is also worth noting that, as the storage time increases, the saturation value of the output field energy decreases mainly due to the dephasing rate γ_s.

Finally we examine in Fig. 5 how the saturation value of output field energy depends on the atomic density. A naive intuition is that this saturation value should be independent of the atomic density because the maximal number of stored photons is just determined by the number of SAs. Fig. 5(a) shows, however, that this saturation value reduces quickly as the atomic density is increased. One main reason is that the Rydberg dephasing rate γ_r is not exactly vanishing (especially when the laser linewidth $\delta\omega_2$ is included) so that the linear absorption contributed by P_2 is always perceptible and becomes more evident for a higher atomic density. Therefore an intermediate density is required to attain a bunch of definite single photons, and more (less) than one photon will be found in a blockade volume for a lower (higher) density. Fig 5(b) and 5(c) show the amplitude profile and the two-photon correlation at the sample exit for three atomic densities. It is clear that the amplitude profile decreases evidently with the increase of the atomic density whereas the two-photon correlation has little change. That indicates that the retrieved field exhibits almost the same photonic statistics though contains different probe photons for different atomic densities. It also worth noting that the two-photon correlation of output pulse becomes more homogenous in a dense enough medium.

IV. CONCLUSIONS

In summary, we have studied the storage and retrieval of a multi-photon probe pulse in cold Rydberg atoms driven into the EIT configuration. By developing the SA model to simulate relevant propagation dynamics, we find a few interesting results absent for the light storage and retrieval in usual EIT media. We find in particular that, in the presence of a vdW interaction, (i) the output probe field is greatly attenuated in intensity yet without suffering an evident temporal broadening; (ii) the output two-photon correlation exhibits an inhomogeneous anti-bunching effect sensitive to the local probe intensity; (iii) the output field energy shows a nonlinear saturation value insensitive to the input field energy. These are all based on the Rydberg blockade effect which sets a rigid limit for the maximal number of stored and retrieved photons and ..... A suitable extension of our results could be explored to prepare various non-classical light fields and manipulating their nonlinear interactions for quantum information applications.

Acknowledgments

This work is supported by National Natural Science Foundation of China (11534002, 11547261, 11704063), Graduate Innovation Fund of Jilin University (2016064), Youth Fund of Liaoning University (LDQN201430), and General Science and Technology Research Plans of Liaoning Educational Bureau (L2014002).

[1] M. Saffman, T. G. Walker, and K. Mølmer, Rev. Mod. Phys. **82**, 2313 (2010).
[2] M. D. Lukin, M. Fleischhauer, R. Côté, L. M. Duan, D. Jaksch, J. I. Cirac, and P. Zoller, Phys. Rev. Lett. **87**, 037901 (2001).
[3] D. Tong, S. M. Farooqi, J. Stanojevic, S. Krishnan, Y.

P. Zhang, R. Côté, E. E. Eyler, and P. L. Gould, Phys. Rev. Lett. **93**, 063001 (2004).
[4] K. Singer, M. Reetz-Lamour, T. Amthor, L. G. Marcassa, and M. Weidemüller, Phys. Rev. Lett. **93**, 163001 (2004).
[5] E. Urban, T. A. Johnson, T. Henage, L. Isenhower, D. D. Yavuz, T. G. Walker, and M. Saffman, Nat. Phys. **5**, 110 (2009).
[6] A. Gaëtan, Y. Miroshnychenko, T. Wilk, A. Chotia, M. Viteau, D. Comparat, P. Pillet, A. Browaeys, and P. Grangier, Nat. Phys. **5**, 115 (2009).
[7] D. Møller, L. B. Madsen, and K. Mølmer, Phys. Rev. Lett. **100**, 170504 (2008).
[8] D. D. Bhaktavatsala Rao and K. Mølmer, Phys. Rev. A **90**, 062319 (2014).
[9] D. D. Bhaktavatsala Rao and K. Mølmer, Phys. Rev. Lett. **111**, 033606 (2013).
[10] X.-D. Tian, Y.-M. Liu, C.-L. Cui, and J.-H. Wu, Phys. Rev. A **92**, 063411 (2015).
[11] I. I. Beterov, M. Saffman, E. A. Yakshina, V. P. Zhukov, D. B. Tretyakov, V. M. Entin, I. I. Ryabtsev, C. W. Mansell, C. MacCormick, S. Bergamini, and M. P. Fedoruk, Phys. Rev. A **88**, 010303 (2013).
[12] M. M. Müller, M. Murphy, S. Montangero, and T. Calarco, Phys. Rev. A **89**, 032334 (2014).
[13] D. D. Bhaktavatsala Rao and K. Mølmer, Phys. Rev. A **89**, 030301 (2014).
[14] M. H. Goerz, E. J. Halperin, J. M. Aytac, C. P. Koch, and K. B. Whaley, Phys. Rev. A **90**, 032329 (2014).
[15] Y. O. Dudin and A. Kuzmich, Science **336**, 887 (2012).
[16] D. Petrosyan, D. D. Bhaktavatsala Rao, and K. Mølmer, Phys. Rev. A **91**, 043402 (2014).
[17] C. Tresp, C. Zimmer, I. Mirgorodskiy, H. Gorniaczyk, A. Paris-Mandoki, and S. Hoerberth, Phys. Rev. Lett. **117**, 223001 (2016).
[18] S. Baur, D. Tiarks, G. Rempe, and S. Durr, Phys. Rev. Lett. **112**, 073901 (2014).
[19] W. Li and I. Lesanovsky, Phys. Rev. A **92**, 043828 (2015)
[20] H. Gorniaczyk, C. Tresp, J. Schmidt, H. Fedder, and S. Hofferberth, Phys. Rev. Lett. **113**, 053601 (2014).
[21] D. Tiarks, S. Baur, K. Schneider, S. Dürr, and G. Rempe, Phys. Rev. Lett. **113**, 053602 (2014).
[22] D. Petrosyan, J. Otterbach, and M. Fleischhauer, Phys. Rev. Lett. **107**, 213601 (2011).
[23] J. D. Pritchard, D. Maxwell, A. Gauguet, K. J. Weatherill, M. P. A. Jones, and C. S. Adams, Phys. Rev. Lett. **105**, 193603 (2010).
[24] T. Peyronel, O. Firstenberg, Q.-Y. Liang, S. Hofferberth, A. V. Gorshkov, T. Pohl, M. D. Lukin, and V. Vuletić, Nature, **488**, 57-60 (2012).
[25] Y.-M. Liu, D. Yan, X.-D. T, C.-L. Cui, and J.-H. Wu, Phys. Rev. A **89**, 033839 (2014).
[26] W. Li, D. Viscor, S. Hofferberth, and I. Lesanovsky, Phys. Rev. Lett. **112**, 243601 (2014).
[27] P. Bienias, S. Choi, O. Firstenberg, M. F. Maghrebi, M. Gullans, M. D. Lukin, A. V. Gorshkov, and H. P. Büchler, Phys. Rev. A **90**, 053804 (2014).
[28] M. F. Maghrebi, M. J. Gullans, P. Bienias, S. Choi, I. Martin, O. Firstenberg, M. D. Lukin, H. P. Büchler, and A. V. Gorshkov, Phys. Rev. Lett. **115**, 123601 (2015).
[29] S. Sevincli, N. Henkel, C. Ates, and T. Pohl, Phys. Rev. Lett. **107**, 153001 (2011).
[30] Y.-M. Liu, X.-D. Tian, X. Wang, D. Yan, and J.-H. Wu, Opt. Lett. **41**, 408 (2016).
[31] E. Distante, A. Padrón-Brito, M. Cristiani, D. Paredes-Barato, and H. de Riedmatten, Phys. Rev. Lett. **117**, 113001 (2016).
[32] D. Maxwell, D. J. Szwer, D. Paredes-Barato, H. Busche, J. D. Pritchard, A. Gauguet, K. J. Weatherill, M. P. A. Jones, and C. S. Adams, Phys. Rev. Lett. **110**, 103001 (2013).
[33] F. Ripka, Y.-H. Chen, R. Löw, and T. Pfau, Phys. Rev. A **93**, 053429 (2016).
[34] J. Ruseckas, I. A. Yu, and G. Juzeliūnas, Phys. Rev. A **95**, 023807 (2017).
[35] A. V. Gorshkov, R. Nath, and T. Pohl, Phys. Rev. Lett. **110**, 153601 (2013).
[36] M. J. Gullans, J. D. Thompson, Y. Wang, Q.-Y. Liang, V. Vuletić, M. D. Lukin, and A. V. Gorshkov, Phys. Rev. Lett. **117**, 113601 (2016).
[37] M. Moos, M. Höning, R. Unanyan, and M. Fleischhauer, Phys. Rev. A **92**, 053846 (2015).
[38] L. Yang, B. He, J.-H. Wu, Z.-Y. Zhang, and M. Xiao, Optica **3**, 1095 (2016).
[39] M. Garttner, S. Whitlock, D. W. Schonleber, and J. Evers, Phys. Rev. A **89**, 063407 (2014).
[40] J.-S. Han, T. Vogt, and W.-H. Li, Phys. Rev. A **94**, 043806 (2016).